Research Paper

Acute telomerase components depletion triggers oxidative stress as an early event previous to telomeric shortening

José Santiago Ibáñez-Cabellos[a,b,c,1], Giselle Pérez-Machado[b,c,1], Marta Seco-Cervera[a,b,c], Ester Berenguer-Pascual[b], José Luis García-Giménez[a,b,c,*], Federico V. Pallardó[a,b,c,*]

[a] Center for Biomedical Network Research on Rare Diseases (CIBERER), Institute of Health Carlos III, Valencia, Spain
[b] Department of Physiology, Faculty of Medicine and Dentistry, University of Valencia, Valencia, Spain
[c] INCLIVA Biomedical Research Institute, Valencia, Spain

ARTICLE INFO

ABSTRACT

Loss of function of dyskerin (DKC1), NOP10 and TIN2 are responsible for different inheritance patterns of Dyskeratosis congenita (DC; ORPHA1775). They are key components of telomerase (DKC1 and NOP10) and shelterin (TIN2), and play an important role in telomere homeostasis. They participate in several fundamental cellular processes by contributing to Dyskeratosis congenita through mechanisms that are not fully understood. Presence of oxidative stress was postulated to result from telomerase ablation. However, the resulting disturbed redox status can promote telomere attrition by generating a vicious circle, which promotes cellular senescence. This fact prompted us to study if acute loss of DKC1, NOP10 and TINF2 can promote redox disequilibrium as an early event when telomere shortening has not yet taken place. We generated siRNA-mediated (*DKC1, NOP10 and TINF2*) cell lines by RNA interference, which was confirmed by mRNA and protein expression analyses. No telomere shortening occurred in any silenced cell line. Depletion of H/ACA ribonucleoproteins DKC1 and NOP10 diminished telomerase activity via TERC down-regulation, and produced alterations in pseudouridylation and ribosomal biogenesis. An increase in the GSSG/GSH ratio, carbonylated proteins and oxidized peroxiredoxin-6 was observed, in addition to MnSOD and TRX1 overexpression in the siRNA DC cells. Likewise, high PARylation levels and high PARP1 protein expression were detected. In contrast, the silenced *TINF2* cells did not alter any evaluated oxidative stress marker. Altogether these findings lead us to conclude that loss of DKC1 and NOP10 functions induces oxidative stress in a telomere shortening independent manner.

1. Introduction

An increasing number of inherited diseases, referred to as telomeropathies, have been correlated with mutations in the genes that encode the proteins required for telomere structure, replication, repair and length maintenance [1], which indicate the genetic complexity of all these syndromes. Telomeres are special functional complexes placed at the end of linear eukaryotic chromosomes, and consist of noncoding tandem repeat DNA sequences and associated shelterin complexes, which together play a dual role in protecting chromosome ends, and in mediating cell proliferation and senescence [2].

The dynamics of telomeres comes under the control of telomerase and shelterin. Telomerase is a reverse transcriptase (hTERT) capable of utilizing an integrated RNA component (hTERC) as a template to add protective tandem telomeric single-strand DNA repeats at the end of chromosomes [3]. Several telomerase-associated accessory proteins like TCAB1, dyskerin (DKC1), NHP2, NOP10, GAR1, among others, guarantee the biological specificity of the enzymatic complex [4]. Shelterin has a core of six proteins, TRF1, TRF2, POT1, Rap1, TPP1 and TIN2, which work together with telomerase in physiological circumstances. In fact the disruption and aberrant activation of either shelterin and/or the telomerase complex lead to deleterious effects for the cell [5].

Dyskeratosis congenita (DC; ORPHA1775), a rare inherited multisystem disorder of premature aging, was the first impaired telomere maintenance syndrome to be described [6]. To date, mutations in 12 genes have been linked to the DC phenotype, many of which share a link to telomere/telomerase biology, such as those that encode for telomerase complex components (TERT, TERC, DKC1, NHP2 and NOP10), shelterin components (TIN2), the proteins involved in T-loop dissociation (RTEL1), telomerase trafficking (TCAB1) and replication

(CTC1) [7,8].

The mutated genes involved in DC result in three modes of transmission: X-linked recessive (X-L), autosomal dominant (AD), and autosomal recessive (AR). Mutations in *DKC1* are related with X-L, the commonest in DC. Mutations in *TERC*, *TERT*, or *TINF2* were found in AD-DC, and *TINF2* is the second most commonly mutated gene in DC. Lastly, *TCAB1*, *NOP10* and *NHP2* have been described in AR-DC [9].

Many DC-related genes perform more than one fundamental cellular function; e.g., DKC1, NOP10, NHP2 are the H/ACA-motif RNA-binding proteins required for the pseudouridylation of rRNAs and snRNAs [10], and alter ribosome and spliceosome functions [11]. Currently, debate continues as to whether the primary cause of DC is a defect in telomerase activity or ribosome biogenesis. In fact there are good arguments for accepting both points of views, and it seems reasonable that both could contribute to the broad range of clinical features found in this syndrome [12].

It is worth bearing in mind that TERT was the first telomeric protein detected in both the mitochondrial matrix and nucleus, and it performs different functions in these two subcellular compartments [13]. Chen and co-workers [14] reinforce the opinion that telomere-related proteins can regulate intermediary metabolism by demonstrating that TIN2 can localize into the mitochondria, where it regulates intermediary metabolism and reactive oxygen species (ROS) production. Altogether, these findings support a link between telomeric proteins and metabolic control by presenting oxidative stress as an additional mechanism by which telomeric proteins can trigger cancer or aging-related phenotypes [14].

In this context, it is noteworthy that DC lymphocytes with different DC mutations (TERT, TIN2, and TERC) have displayed a stressed phenotype characterized by high levels of ROS, DNA damage response (DDR), apoptotic markers and proliferative defects [15]. The opposite has also been postulated; oxidative stress can promote telomere attrition, which suggests a potential feedback loop to sustain elevated ROS and to favor entry into senescence. In fact oxidative stress has been suggested to be a major cause of telomere shortening [15]. So although it has been contended that the role of DDR and elevation of ROS are secondary to telomere shortening in DC [16], the possibility of oxidative stress contributing to the physiopathology of the disease as an early contributor cannot be ruled out.

Among the proteins involved in the pathogenesis of DC, DKC1 has been the subject of the vast majority of depletion studies [17,18]. However, the effects of the targeted depletion of other H/ACA proteins, like NOP10, have been poorly characterized. Likewise, the roles of TIN2 mutations in telomere maintenance, DDR and antioxidant defense are still a challenge that requires further research.

We aim to silence essential genes (*DKC1*, *NOP10* and *TINF2*) in Hela cells, as was previously done in other studies [19–21], for the functionality of telomerase and shelterin complexes, which are involved in several inheritance patterns of DC, in order to evaluate their role in oxidative stress, antioxidant responses and DDR without interfering with telomere length.

2. Experimental procedures

2.1. Cell culture

HeLa cells (American Type Culture Collection, Manassas, VA. USA) were grown in DMEM (Gibco Life Technologies, Karlsruhe, Germany), supplemented with 10% fetal bovine serum (FBS) and 1% antibiotics (100 U mL^{-1} penicillin/100 µg mL^{-1} streptomycin) (Sigma-Aldrich, St. Louis, MO. USA) in a 5% CO_2 incubator at 37 °C.

2.2. siRNA transfections

HeLa cells were seeded at a density of 2×10^5 per well in six-well plates that contained 2 mL of DMEM medium supplemented with 10%

FCS with no antibiotic. After 24 h, cells were subjected to two sequential transfections, separated by a 24-h interval. Transfections were carried out using validated siRNA (siTARGET) for *DKC1 (siDKC1)*, *NOP10 (siNOP10)* and *TINF2 (siTINF2)* mRNA (ID: s4111, ID: 215701, and ID: s25355, Ambion, CO, USA) at 100 nM with Lipofectamine RNAiMAX (Invitrogen, Carlsbad, CA, USA), according to the manufacturer's protocol. Non targeting siRNA (Cat: AM4635, Silencer Negative Control siRNA #1, Ambion), under the same transfection conditions, was considered to be siCONTROL, and a HeLa wild-type was used as the CONTROL. Cells were harvested 48 h after the initial transfection for the next experiments. RNAi efficacy was assessed by quantitative polymerase chain reaction (qPCR) and Western blotting (WB).

2.3. Quantitative RT–PCR

For the reverse transcription reactions (RT), 200 ng of the purified total RNA were reverse-transcribed using random hexamers with the High-Capacity cDNA Archive kit (Applied Biosystems, P/N: 4322171, Foster City, USA) according to the manufacturer's protocol. The RT conditions comprised an initial incubation step at 25 °C for 10 min to allow random hexamers annealing, followed by cDNA synthesis at 37 °C for 120 min, and a final inactivation step for 5 min at 95 °C.

The mRNA levels were determined by a quantitative real-time PCR analysis in an ABI Prism 7900HT Fast Real-Time PCR System (Applied Biosystems, Foster City, CA, USA). The gene-specific primer pairs and probes for *DKC1* (Hs00154737_m1), *NOP10* (Hs00430282_m1), *TINF2* (Hs01554309_g1), *TERC* (Hs03454202_s1), *TERT* (Hs00972650_m1), Superoxide Dismutase 2 (*SOD2*, Hs00167309_m1), Thioredoxin 1 (*TRX1*, Hs00917067_m1), Thioredoxin 2 (*TRX2*, Hs00912509_g1), Poly (ADP-ribose) Polymerase 1 (*PARP1*, Hs00242302_m1), oxoguanine glycosylase (*oGG1*, Hs00213454_m1), Xeroderma Pigmentosum Complementation Group A (*XPA*, Hs00166045_m1), Werner (*WRN*, Hs01087915_m1), *RAD51* (Hs00947967_m1), *RAD53* (Hs00200485_m1), *18S* (Hs0300 3631_g1), and *GAPDH* (Glyceraldehyde-3-phosphate dehydrogenase, Hs02758991_g1) were used together with 1x TaqMan® Universal PCR Master Mix (Applied Biosystems, P/N 4304437, Foster City, CA, USA) and 1 µL of the reverse-transcribed sample RNA in 10 µL reaction volumes. The PCR conditions were 95 °C for 10 min, followed by 40 cycles at 95 °C for 15 s and 60 °C for 1 min. GAPDH was chosen as the endogenous reference for the normalization of the qRT-PCR-based expression analysis. Each sample was analyzed in triplicate, and the relative quantification of mRNAs was calculated by the $2^{-\Delta\Delta CT}$ method [22].

2.4. Immunoblotting Western blot

Protein extracts were obtained from the HeLa cells lysed in ice using lysis buffer (20 mM Hepes, pH 7.4, 1% Triton X-100, 100 mM NaCl, 50 mM NaF, 10 mM β-glycerophosphate, 1 mM sodium orthovanadate, 1 mM phenylmethanesulfonyl fluoride (PMSF), and the protein protease inhibitor cocktail (Roche Diagnostics, Barcelona, Spain)). The resultant suspension was centrifuged at 13,000*g* for 10 min at 4 °C and supernatants were stored at − 80 °C until use. Protein content was determined by the Bradford method [23].

Proteins were prepared in LDS sample buffer (Tris 40 mM, EDTA, bromophenol blue 0.01%, sucrose 40%, SDS 4%, β-mercaptoethanol 10%) and heated to 95 °C for 5 min. Proteins were resolved by sodium dodecyl sulfate–polyacrylamide (12%) gel electrophoresis (SDS–PAGE) at 100 V for 2 h. They were then transferred to nitrocellulose membranes (Whatman GmbH, Dassel, Germany). Following transference, the membrane was blocked in 5% skimmed milk in 0.1% Tween-20 (Sigma-Aldrich) and phosphate-buffered saline (PBS). Membrane slices were incubated with specific monoclonal antibodies: Dyskerin (DKC1, 1:1000, Santa Cruz Biotechnology, Texas, USA), NOP10 (1:1000, Santa Cruz Biotechnology, Texas, USA), TIN2 (1:1000, Santa Cruz Biotechnology, Texas, USA), a sulfonic acid form of PRDX6 (PRDX6-SO$_3$H, 1:1000, Abcam, Cambridge, UK), manganese superoxide

dismutase (MnSOD, 1:1000, Stressgen, Ann Arbor, MI, USA), thioredoxin 1 (TRX1, 1:1000, Abcam, Cambridge, UK), thioredoxin 2 (TRX2, 1:1000, Abcam, Cambridge, UK) and β-actin (1:1000, Santa Cruz BioTech, USA) and histone H3 (1:5000) antibodies as the loading controls. Then blots were washed with TBS-Tween, and incubated with a secondary mouse, rabbit or goat antibody conjugated with horseradish peroxidase-linked. The membrane was incubated for 50 min at room temperature and under constant agitation. Finally, the membrane was washed 3×5 min with TBS-Tween. Protein bands were visualized with ECL Western blotting detection reagents (GE Healthcare, UK) and membranes were revealed by image reader LAS-4000 (General Electrics, Healthcare, UK). The Western blot results were assessed visually by making comparisons between the bands in different lanes, and also were scanned. The relative optical density (ROD) was quantified by Image J (National Institutes of Health, Bethesda, MD, USA). The ROD ratio was calibrated as a percentage with siCONTROL or CONTROL, designated as 100%.

2.5. Cell viability assay

Apoptosis was determined by the Annexin-V FITC kit (Immunostep, Salamanca, Spain) following the manufacturer specifications. Silenced cells and controls were resuspended in Annexin-V buffer and stained with Annexin-V- FITC and propidium iodide (PI) for 15 min in the dark. Then the stained cells were analyzed by flow cytometry in a FACS-Verse cytometer (Beckton Dickinson, San Jose, CA, USA) and with the Infinicyt software (Cytognos, Santa Marta de Tormes, Salamanca, Spain).

2.6. Cell cycle

The cell cycle was determined by the PI/RNASE Solution kit (Immunostep, Salamanca, Spain) following the manufacturer specifications. All the cell lines were resuspended in 70% ethanol for 1 h at 4 °C in the dark. Then cells were washed and stained with PI/RNASE for 15 min in the dark. Afterward the stained cells were analyzed by flow cytometry in a FACS-Verse cytometer (Beckton Dickinson, San Jose, CA, USA) and with the Infinicyt software (Cytognos, Santa Marta de Tormes, Salamanca, Spain).

2.7. Telomerase activity assay

Telomerase activity was measured using the real-time quantitative telomeric repeat amplification protocol (RTQ-TRAP assay). The silenced HeLa cells were harvested using trypsin-EDTA (Gibco/Invitrogen, Carlsbad, CA, USA) and pelleted by centrifugation at $5000 \times g$ for 3 min at 4 °C. Protein extracts were diluted to a concentration of 1 mg/mL protein with lysis buffer.

The RTQ-TRAP assay was performed in two steps: (i) telomerase-mediated extension of the forward primer (TS: 5′-AATCCGTCGAGCAGAGTT-3′), (Oswel, Southampton, UK) and (ii) a PCR amplification step. In detail, 1 µg of the telomerase extract was incubated for 20 min at 25 °C in the reaction mix that contained the LightCycler 480 SYBR Green I Master (Roche Diagnostics) mix, 5 pmol of primer TS and 1.25 pmol of primer ACX (5′ GCGCGGCTTACCCTTACCCTTACCCTAACC- 3′).

The second step was performed in a LightCycler System 480 (Roche Diagnostics, Mannheim, Germany) under the following cycle conditions: 95 °C for 5 min, followed by 40 cycles (95 °C for 30 s, 55 °C for 30 s, and 72 °C for 30 s) and one cycle that corresponded to the melting curve.

Controls such as (i) telomerase positive; (ii) lysis buffer; and (iii) nuclease-free water were included in the experiments. A standard curve was also generated using serial dilutions of HeLa cells (10,000, 1000, 100, 10, 1, and 0.1 HeLa cells). Presence of the internal telomerase assay standard allowed us to determine presence of Taq polymerase

inhibitors' internal standards (amplified with the same primers as telomerase). The TRAP internal control, TSNT (5-AATCCGTCGAGCAGAGTTAAAAGGCCGAGAAGCGAT- 3) at 0.01 pmol was amplified by 7.5 pmol of primer TS and its own dedicated return primer, NT (5-ATCGCTTCTCGGCCTTTT-3′). Each sample was analyzed in duplicate in three independent experiments. Telomerase activity was comparatively assessed based on Ct, and was determined as the percentage of remaining telomerase activity:

Activity Remaining (%) = $1/1.8 \ \Delta^{Ct} \times 100$

ΔCt = Ct Treatment − Ct Control

2.8. Telomerase length assay

DNA was isolated using the Qiagen DNeasy Blood & Tissue Kit (Hilden, Germany) following the manufacturer's instructions for cellular material. Telomere length was measured and compared as the telomere-to-single copy gene ratio (T/S) by quantitative real-time PCR. Primer sequences, the concentrations for telomere and the 36B4 gene, and as the PCR conditions, and quantification were as described by Cawthon et al. [24], with some modifications. Each sample was analyzed in triplicate using 10 ng of DNA, 7 µL of H2O, 10 µL of master mix, and 2 µL oligos per sample. For each standard curve, a reference DNA sample (1691112, Roche Diagnostics, Barcelona, Spain) was diluted serially in water at the 1:10 dilution, where the range of concentrations started from 200 to 0.2 ng in 1 µL. The thermal cycling profile was: first one cycle of 15 min at 95 °C, followed by 45 cycles of 10 s at 95 °C, 5 s at 55 °C and 11 s at 72 °C.

2.9. Measuring the GSSG/GSH ratio

The reduced glutathione (GSH) and oxidized glutathione (GSSG) levels were studied with the Glutathione Fluorescent Detection Kit (Arbor Assays, Ann Arbor, Michigan USA) following the manufacturer's instructions for cellular material. Briefly, $2 \cdot 10^5$ cells were lysed in cold 5% sulphosalicylic acid and centrifuged at 14,000g to separate proteins. The supernatant that contained GSH and GSSG was reacted with ThioStar reagent to produce a fluorescent product (λ emission 510 nm, λ excitation 390 nm). Fluorescence readings were taken using fluorescent emission at 510 nm and with excitation at 390 nm in a fluorimeter spectraMAX GEMINI (Molecular Devices, Sunnyvale, USA). The GSSG levels were calculated using the formula GSSG = (Total GSH- Free GSH)/2.

2.10. Immunodetection of the protein-bound carbonyl groups by Dot blot

Proteins were derivatized to 2,4-dinitrophenylhydrazone (DNP-hydrazone) by its reaction with 2,4-dinitrophenylhidrazine (DNPH), following the procedure of Shacter et al. [25]. Briefly, 5 µL of proteins were denatured with 12% SDS. Protein solutions were treated with DNPH 10 mM in 10% (v/v) trifluoroacetic acid. Samples were transferred to a nitrocellulose membrane. Then the membrane was blocked with 5% bovine serum albumin (BSA) in phosphate-buffered saline (PBS) – 0.1% Tween for 1 h and incubated with the anti-DNP antibody as described by the manufacturer of the OxyBlot kit (OxyBlot Protein Oxidation Detection kit; Millipore, Billerica, MA, USA). Protein bands were visualized with the ECL Western blotting detection reagents (GE Healthcare, UK) and membranes were revealed by image reader LAS-4000 (General Electrics, Healthcare, UK).

2.11. Histone variant H2A.X phosphorylated on Ser139 (γ-H2A.X) analyzed by flow-cytometry

HeLa cells (1×10^6 cells/mL) were fixed in 4% paraformaldehyde for 15 min at room temperature. Samples, which were mixed with PBS,

were permeabilized with 0.5% Triton X-100 for 10 min. Subsequently, cell pellets were resuspended in 50 μL of Alexa Fluor 488 Mouse anti-γ-H2A.X (pS139) (1:120 dilution in PBS) (BD Pharmingen, New Jersey, USA) and incubated for 1 h at 37 °C. Finally, they were resuspended in PBS and analyzed in a FACS flow cytometer (BD FACSverse, New Jersey, USA); 5000 events were recorded within the characteristic flames-shaped region in the forward scatter region/side scatter (FSC/SSC) dot plot.

The control samples were evaluated in each experiment. The fluorescence of the untreated cells was recorded to determine the level of the background fluorescence for the negative control cells, while the cells treated with 0.5 mM H_2O_2 (1 h at 37 °C) were included as a positive control. The levels of γ-H2A.X were evaluated and compared for each cellular model at steady-state (without H_2O_2 treatment) and after induction of DNA damage using 0.5 mM H_2O_2 during 1 h at 37 °C. Results were expressed as a percentage of the double-strand breaks (DSB).

2.12. Poly(ADP-ribosyl)ation (PARylation) analyzed by flow-cytometry

The PAR reaction was also evaluated by flow cytometry with a similar procedure to that described above, except for modifications in relation to experimental conditions and the antibodies used for the PAR detection. Briefly, the levels of PARylation were evaluated and compared for each cellular model at steady-state (without etoposide treatment) and after induction of DNA damage using 200 μM etoposide during 1 h at 37 °C. Cells were stained with Anti-Poly (ADP-ribose) Mouse Monoclonal Antibody (1:150 dilution in PBS) (Trevigen, Gaithersburg, MD, USA) and incubated overnight at 4 °C. The cells resuspended in Alexa Fluor goat anti-mouse 488 IgG (1:530 dilution in PBS) (H+L) (Life Technologies, Rockford, USA) were incubated for 1 h at 37 °C. The positive control of the PAR signal was obtained by incubating cells with 200 μM of etoposide (1 h at 37 °C) (Sigma-Aldrich, Saint Louis, Missouri, USA). Moreover, the negative controls were obtained by incubating cells only with secondary goat anti-mouse 488 IgG (1:530 dilution in PBS) (H+L) (Life Technologies, Rockford, USA) for 1 h at 37 °C; 5000 event files for each sample were acquired individually in a FACS flow cytometer (BD FACSverse, New Jersey, USA) [26].

2.13. Pseudouridylation assay on endogenous 28 S rRNA

The total cellular RNA from the silenced cells was modified with 1-Cyclohexyl-3-(2-morpholinoethyl) carbodiimide metho-p-toluenesulfonate (CMCT, Aldrich (Milwaukee, WI, USA) as previously described [27]. Briefly, BEU Buffer (7 M Urea, 4 mM EDTA, 50 mM Bicine-pH 8.5, final buffer pH = 8.929.0) and CMCT 1 M (Sigma–Aldrich) were added to 3 μg of RNA. Samples were incubated for 20 min at 37 °C and precipitated by adding Pellet Paint Co-Precipitant (Merck), sodium acetate 3 M (pH 5.5) and ethanol. Pellets were resuspended in sodium carbonate buffer, pH 10.4 (50 mM sodium carbonate and 2 mM EDTA), and were then incubated at 37 °C for 4 h. At the end of the reaction, RNA was precipitated by adding Pellet Paint Co- Precipitant, 3 M sodium acetate, and ethanol. Pellets, previously washed with 70% ethanol, were resuspended in water and quantified by a NanoDrop.

The reverse transcription reaction was carried out in a final 20 μL mixture; 200 ng of RNA, 0.2 μM of 28 S RNA specific reverse primer (5´-ATTATGCTGAGTGATATCCCATCGAAGGATCAAAAAGCGA-3´) and the Maxima First-Strand cDNA Synthesis kit, were mixed and incubated at 50 °C for 10 min to allow specific reverse primer annealing.

2.13.1. Real-time PCR reaction

The RT mixture was used as a template for the subsequent Real-time PCR analysis, which was performed in a Gene Amp 7000 Sequence Detection System (Applied Biosystems) by the Syber-green (Applied Biosystems) approach. The used set of primers (28 S) comprised: primer

Forward 5- GTGTCAGAAAAGTTACCACA-3; primer Reverse 5´-ATTATGCTGAGTGATATCCC-3´. TERC was used as an endogenous control. Each sample was analyzed in triplicate, and the relative gene expression was calculated according to the $2^{\Delta\Delta Ct}$ method [22].

2.14. Statistical analysis

All the experiments were performed at least 3 times for statistical significance. The results represent mean ± SD of three independent experiments. A Mann–Whitney *U* test was applied to compare the data among the siTARGET, siCONTROL, and CONTROL cell lines to assess statistical significance. P-values under 0.05 were considered significant. The error bars inside graphs represent the standard deviation of the replicate samples. A statistical data analysis was performed using the GraphPad Software v6.0.

3. Results

3.1. Successful generation of the siDKC1, siNOP10 and siTINF2 cellular models

In order to ensure adequate cellular models to conduct our study, we measured the gene expression and protein levels of the targeted genes, as well as telomere length, 48 h after gene silencing. The levels of *DKC1*, *NOP10* and *TINF2* mRNA lowered by more than 90% compared to the siCONTROL and CONTROL groups (Figs. 1A, 1B, 1C). In accordance with the gene expression results, we observed a reduction of up to 40% in the DKC1, NOP10, and TIN2 protein levels by Western blot analysis (Fig. 1D and Supplementary Fig. S1).

The decreasing *DKC1* and *NOP10* mRNA levels concomitantly lowered *TERC* levels and diminished telomerase activity (Fig. 2A). The siDKC1 and siNOP10 cells showed the most pronounced reduction of telomerase activity (Fig. 2C). In contrast, *TINF2* depletion affected neither the expression of telomerase subunits nor their enzymatic activity (see Figs. 2A, 2B, 2C). No effects on TERT expression were found in any of the three silenced genes (Fig. 2B). We also measured telomere length and did not observe any telomere shortening (Fig. 2D), nor did we detect differences in viability (Supplementary Fig. S2A) and cell cycle (Supplementary Fig. S2B) among the various groups.

A real-time PCR assay was used to detect pseudouridylation levels in endogenous 28 S rRNA. We found that the lowered DKC1 and NOP10 expression actually reduced in vitro rRNA pseudouridylation (Fig. 2F). Probably as a direct result of this, the mature 18S rRNA levels were lower in the cells depleted of the DKC1 and NOP10 proteins (Fig. 2E). However, neither pseudouridylation nor 18 S rRNA synthesis was affected after *TINF2* silencing (Figs. 2E, 2F).

3.2. Oxidative stress is a feature of siRNA-mediated (DKC1, NOP10 and TINF2) gene-silencing cellular models

We measured the oxidative stress profile in the siRNA cell models by measuring different oxidative stress markers. Protein oxidation was determined by measuring the carbonylated protein levels. The Dot Blot results showed an increase in the carbonylated proteins in the siDKC1 and siNOP10 cells, but no differences were observed in the siTINF2 cells compared to the CONTROL (Fig. 3A).

The analysis of the PRDX6-SO$_3$H, a bifunctional enzyme with glutathione peroxidase and phospholipase A$_2$ activities, was done by Western blot. Our results showed high levels of PRDX6-SO$_3$H in the siDKC1 and siNOP10 cells, while the siTINF2 cells revealed no differences (Fig. 3B).

Finally, we calculated the GSSG/GSH ratio, which informs about the redox status of cells. Our results showed high GSSG/GSH ratio levels in the siDKC1 and siNOP10 cells, while the siTINF2 cells revealed no differences compared to the control cells (Fig. 3B and Fig. 3C).
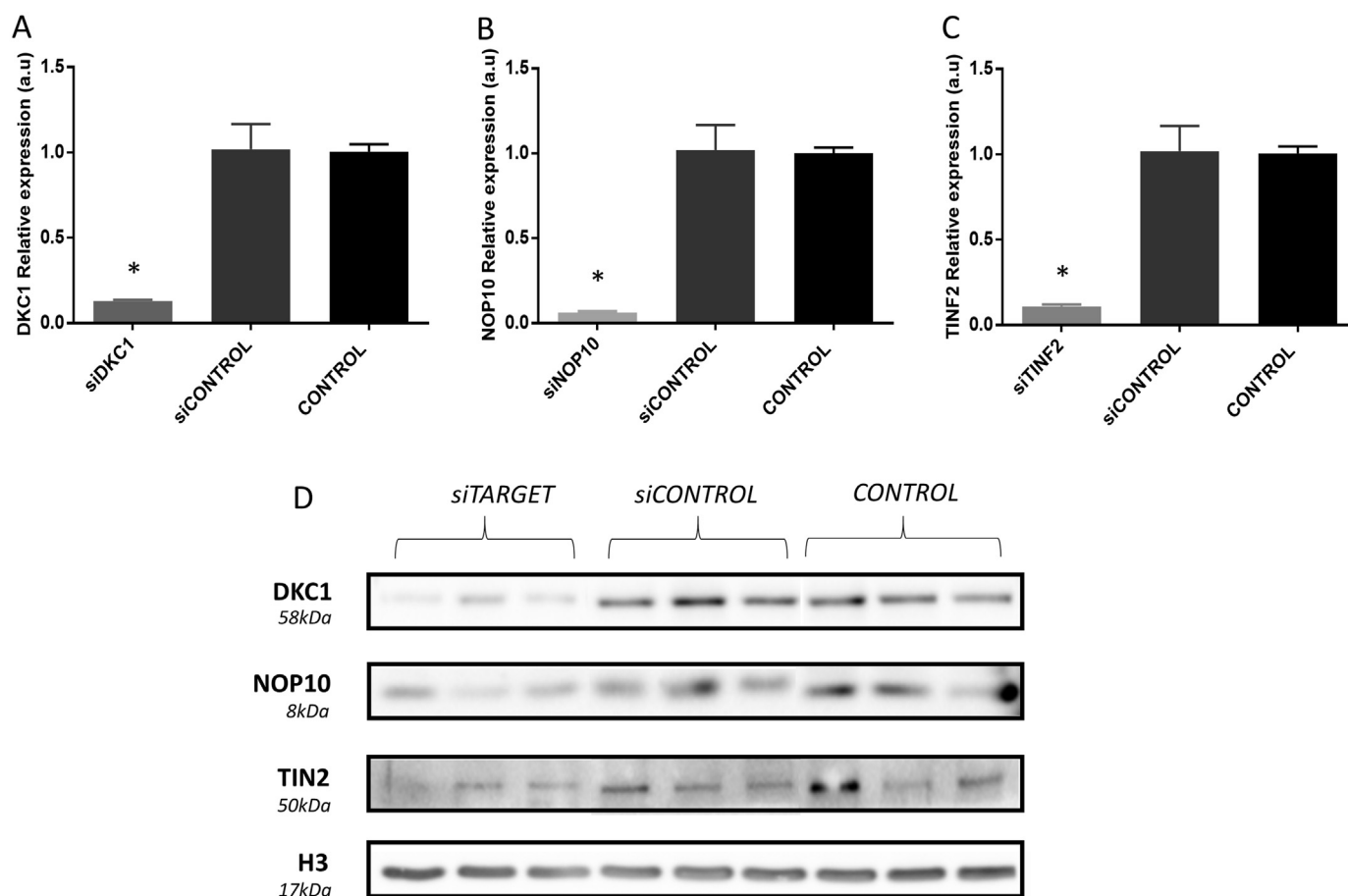
Fig. 1. Analysis of the DC cell models (siDKC1, siNOP10, siTINF2) generated by siRNA technology 48 h after the first transfection. **A)** The *DKC1* mRNA levels evaluated by RT-qPCR. **B)** The *NOP10* mRNA levels evaluated by RT-qPCR. **C)** The *TINF2* mRNA levels evaluated by RT-qPCR. The expression was compared to *GAPDH* as a gene for normalization. Bars represent the mean ± SD of three independent experiments and statistical significance refers to the value of the CONTROL samples under each condition (*p < 0.05). **D)** The Western blot analysis of Dyskerin, NOP10, and TIN2. The expression was compared to H3 as a protein for normalization (Densitometry data are shown in Supplementary Fig. S1). There were three independent experiments per group.

3.3. Antioxidant enzyme activities are altered in DC cellular models

Antioxidant defenses were characterized by studying a series of antioxidant enzymes by RT-qPCR and Western blot. The RT-qPCR results showed an increase in the mitochondrial *SOD2* mRNA levels in siDKC1 and siNOP10, but no significant differences were observed for siTINF2 (Fig. 4A). The MnSOD protein levels increased only in the siNOP10 cells (Fig. 4D and Supplementary Fig. S3A), which agree with the results obtained for *SOD2* mRNA expression (Fig. 4A).

We also studied the mRNA expression levels of *TRX2* and *TRX1* in the siRNA-transfected cells. The results showed that the siDKC1 and siNOP10 cells exhibited *TRX1* mRNA overexpression, which remained unchanged for the siTINF2 cells (Fig. 4B). Moreover, the mRNA content of *TRX2* was up-regulated in the siNOP10 cells and down-regulated in the siTINF2 cells (Fig. 4C). A Western blot analysis of these enzymes confirmed TRX1 overexpression in siNOP10 (Fig. 4D and Supplementary Fig. S3B), but indicated no change in siDKC1 and siTINF2. Otherwise, the TRX2 protein levels lowered in the siTINF2 cells (Fig. 4D and Supplementary Fig. S3C), but not in the other DC cellular models.

We also analyzed catalase (*CAT*) and superoxide dismutase 1 (*SOD1*), but we detected no changes in the expression of these proteins in all the generated siRNA DC cellular models (data not shown).

3.4. DNA damage response is affected in DC cellular models

An increase in oxidative stress can produce DNA damage. Therefore,

we wondered whether a reduced expression of DKC1, NOP10 and TIN2 could influence DDR. To this end, we examined the post-translational marks related with DNA damage by flow cytometry: I) the histone variant H2A.X phosphorylated on Ser139 (γ-H2A.X) foci and II) the protein poly ADP-ribosylation (PARylation) levels.

The number of γ-H2A.X-positive cells (Fig. 5A) and PARylation levels (Fig. 5C) did not reveal any changes at the steady-state levels for any of the three DC cellular models. Nor did we find any change in these markers when we promoted DNA damage by using a treatment of 0.5 mM H$_2$O$_2$ during 1 h (Fig. 5B), although the PARylation levels significantly increased after the treatment of siDKC and siNOP10 cells using 200 μM of etoposide during 1 h. Changes in protein PARylation in siTINF2 cells were not observed in etoposide-treated siTNF2 cells (Fig. 5D).

As we observed an increase in the PARylation levels, we decided to analyze *PARP1* gene expression, either with or without treatment with etoposide, and we found no changes in *PARP1* expression under the basal conditions (Fig. 5E). However, a significant increase in *PARP1* expression was detected in DKC1 and NOP10 silenced cell lines after challenge (Fig. 5F). These results indicate that increased susceptibility to DNA damage occurs when DKC1 and NOP10 are silenced.

We also analyzed the expression of the key genes that participate in DNA damage sensing, such as RAD53, during base excision repair (BER), such as *oGG1*, and nucleotide excision repair (NER), such as a *XPA*. We also evaluated the expression of the genes that participate in homologous recombination, such as RAD51 and bi-functional helicase, in homologous recombination and the non-homologous end joining
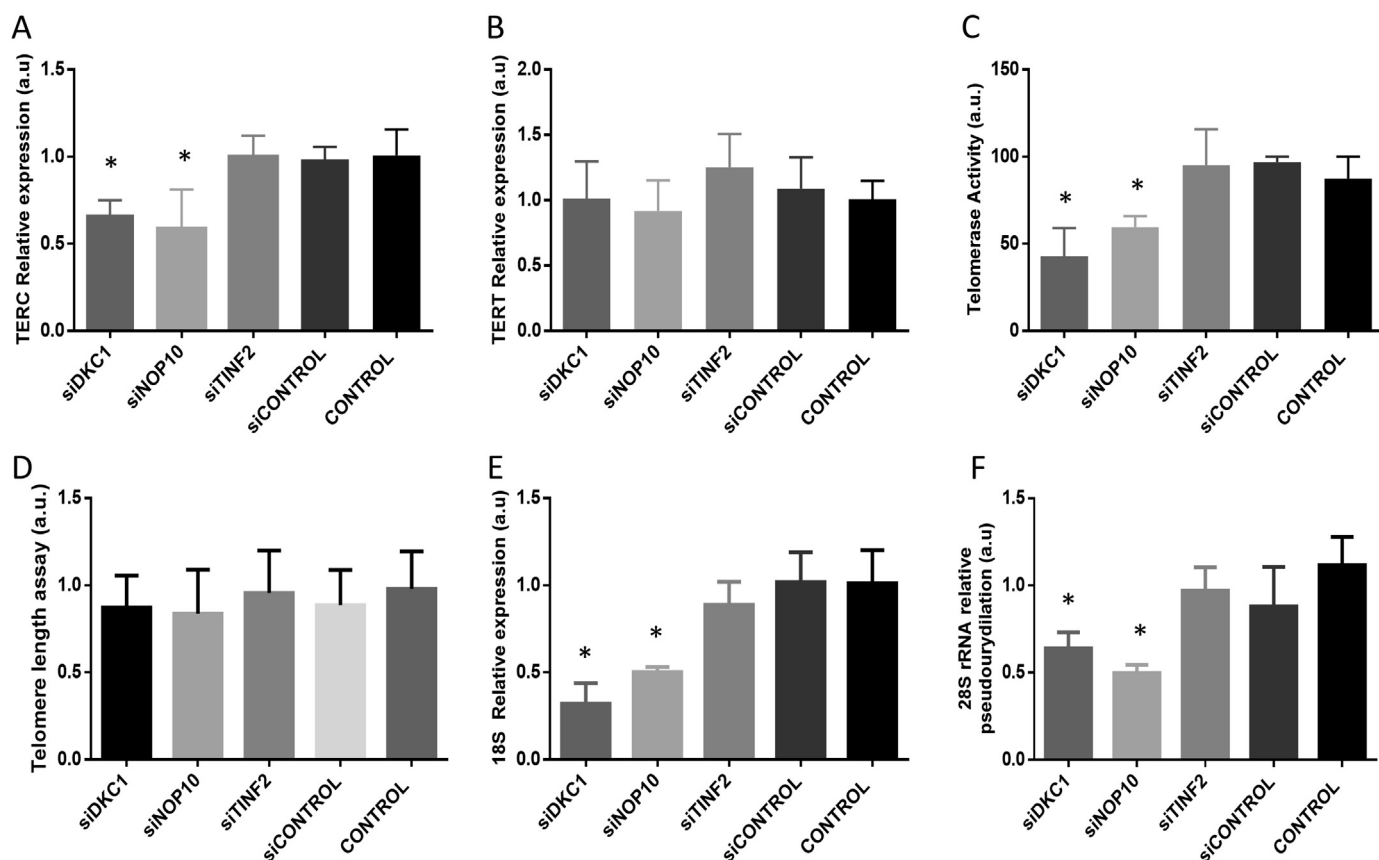
Fig. 2. Characterization of the DC cell models (siDKC1, siNOP10, siTINF2). **A)** The *TERC* gene relative expression in different cell models. The expression was compared to *GAPDH* as a gene for normalization. **B)** The *TERT* gene relative expression in the different cell models. The expression was compared to *GAPDH* as a gene for normalization. **C)** Telomerase activity in the different populations. **D)** Telomere length measured as the telomere-to-single copy gene ratio (T/S). **E)** The *18S* ribosomal RNA relative expression in the different cell models. The expression was compared to *GAPDH* as a gene for normalization. **F)** *28S* ribosomal RNA relative pseudouridylation in the different cell models. All the results were obtained by RT-qPCR. Bars represent the mean ± SD of three independent experiments and statistical significance refers to the value of the CONTROL samples under each condition (*$p < 0.05$).

WRN protein. However after the qRT-PCR analysis, we observed no changes in the expression of most of these genes (Supplementary Fig. S4). The only changes we found were in *RAD51* when NOP10 was silenced, which suggests that homologous recombination was affected (Supplementary Fig. S4).

4. Discussion

Nowadays there is no doubt that the malfunctioning genes involved in telomere biology and/or ribosome processing, such as *DKC1, NOP10* and *TINF2,* underlie the genotype of many telomeropathies and drive their clinical features [7]. It is also accepted that the mechanisms which contribute to DC are not fully understood [28,29].

Growing evidence indicates that oxidative stress and DDR are closely linked with telomere homeostasis, and with the onset of many forms of DC [30,31].

Several authors have paid attention to oxidative stress, and have observed that the mutations of some DC genes are associated with both an increase in ROS levels and a lowered expression of the antioxidant enzymes in DC patients' cells [12,32,33]. These results support a mechanism whereby telomere dysfunction initiates a DDR and creates a pro-oxidant environment [12,15]. In turn, other findings have underpinned a model in which disturbances to oxidative pathways can promote telomere attrition, which suggests a positive feedback loop to sustain elevated ROS and to favor entry into senescence [15]. Moreover, our group previously demonstrated that the in vitro activity of telomerase can be modulated by a redox environment, and Fouquerel et al. have described how oxidative lesion 8-oxo-7,8-dihydro-2'-deoxyguanine (8-oxoG) regulates telomere elongation by human telomerase

[34]. Nonetheless, variations in redox equilibrium have been generally interpreted as a result of telomerase ablation [35,36].

A further issue to consider is that fibroblasts from DC patients probably develop compensatory mechanisms when the expression of DC genes is acutely interrupted [32]. Indeed, although the fibroblasts obtained from DC patients, and those obtained by RNAi technology, display similar biological events (e.g. p53 activation, telomerase inhibition, and cellular senescence induction), the molecular mechanisms that take place may differ depending on telomere length [31,32].

Findings in a zebrafish model of DC, which contained mutations in *nop10,* confirmed that other events, e.g. failure in ribosome biogenesis and p53 deregulation, can contribute to the DC phenotype prior to telomere shortening [37].

As gene silencing by "small interfering RNAs" (siRNAs) is a powerful tool to identify the gene function [38], we hypothesized that a transient knockdown of the genes involved in several inheritance patterns of DC, such as *DKC1, NOP10 and TINF2*, could allow us to unravel if the acute depletion of these genes triggers a redox disequilibrium, even when telomere shortening has not yet taken place.

Our results corroborated that there were no differences in telomere length in any of the siRNAs DC models 48 h after gene silencing, which rules out the notion that telomere shortening is a mechanism involved in the siRNA DC stressed phenotype.

As expected, the siDKC1 and siNOP10 cells produced low levels of TERC, and diminished telomerase activity. DKC1 and NOP10, as H/ACA ribonucleoproteins, exert most of their influence on the cell via H/ACA RNA binding [39]. TERC contains a H/ACA snoRNA-like sequence at its 3´-end, which binds these H/ACA proteins. Therefore, any dysfunction leads to failed trafficking, accumulation and telomerase
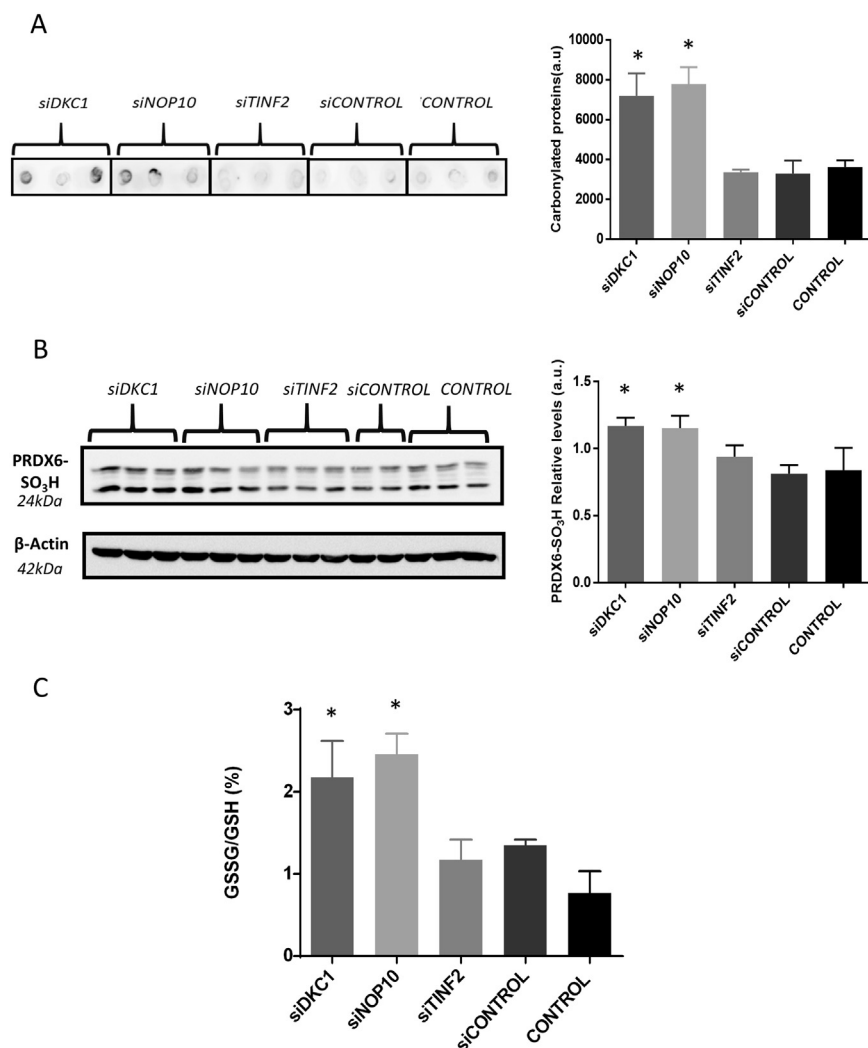
A

B

C

Fig. 3. Analysis of the oxidative stress parameters in the silenced HeLa cells. **A)** A Dot Blot analysis of the DNPH-derivatized proteins to detect carbonylated proteins (OxyBlot Protein Oxidation Detection kit, Millipore). Carbonylation marks were densitometered with ImageJ (National Institutes of Health, USA), values were normalized to the protein total content and compared to the CONTROL values. The results are shown as arbitrary units (a.u.), normalized to the control samples. There were three independent experiments per group. **B)** The Western blot analysis of Prdx6-SO_3H. The expression was compared to β-Actin as a protein for normalization. Prdx6-SO_3H specific bands were densitometered with ImageJ (National Institutes of Health, USA), values were normalized to β-Actin and compared to the CONTROL values. The results are shown as arbitrary units (a.u.). There were three independent experiments per group. **C)** The GSSG/GSH ratio was quantified by the GSH kit (DetectX, Glutathione Fluorescent Detection kit", ArborAssays). Bars represent the mean ± SD of three independent experiments and statistical significance refers to the value of the CONTROL samples under each condition (*$p < 0.05$).

biogenesis [40–43]. The loss of function of any of these proteins reduces TERC stability, and usually diminishes telomerase activity [39,43].

TIN2 has been proposed as a central component of the shelterin complex by helping to recruit the telomerase component (TERT) [44]. TIN2 is also a PARP modulator in the TRF1 complex, which also explains how TIN2 contributes to telomere length regulation. However, TERC has been reported to be the limiting factor for telomerase activity and telomere maintenance [45]. Although TIN2 contributes to the phenotype when associated with DC mutations, it is accepted that TIN2 loss has no effect on TERC expression levels [15,46,47] and total telomerase activity [48]. The results obtained in our siTINF2 model also confirmed the observations made by Yang et al. [48].

DKC1 and NOP10 are proteins that are also required for 18 S rRNA synthesis, and also for rRNA and snRNAs pseudouridine modifications, which are considered the commonest and evolutionarily conserved modifications of nucleotides in eukaryotic RNAs [20,39]. Although the role of modified residues in these RNAs is not fully understood, pseudouridines appear to be important for rRNA stability and function, and also for snRNP assembly and function [10].

Previous HPLC analyses of rRNA have confirmed that the cells transfected with DKC1-specific siRNAs decrease pseudouridylation after detecting a lower rRNA ψ/C ratio (where ψ is a C-glycoside isomer of uridine and C cytosine) for 18 S RNA, and also for 28 S RNA but to a lesser extent [49]. It has also been reported that mutant zebrafish with a low nop10 expression show 18 S rRNA processing defects and the collapse of the small ribosomal subunit, while their role in telomere

maintenance does not contribute to DC until later in life [37].

It is noteworthy that DKC1 and NOP10 depletions may also induce low levels of other H/ACA RNAs and H/ACA snoRNPs, as well as other protein functions [4,10,31,50,51]. Therefore, it seems reasonable to believe that many of the effects we found herein were mediated by the deregulation of H/ACA RNAs and other several proteins after DKC1 and NOP10 depletion, rather than being due to the single loss of silenced proteins.

One of the pleiotropic effects found in our siRNA DC models is increased oxidative stress. In line with this, PRDX6-SO_3H and carbonylated proteins further confirmed increased oxidative stress in siDKC1 and siNOP10 [52]. The detection of high GSSG levels and an increase in the GSSG/GSH ratio also corroborated oxidative stress in the siDCK1 and siNOP10 cellular models. These results agree with previous studies in DC cells [33]. For siTINF2 no changes were observed, these results are in agreement with previous studies [14].

DC cells signal a DDR through p53 and its downstream mediator, p21(WAF/CIP), which is accompanied by a rise in superoxide and GSSG, both of which are indicators of oxidative stress [16]. Oxidative stress is defined as the imbalance between reactive oxygen and nitrogen species production and antioxidant capacity. Therefore, we also studied the expression of antioxidant enzymes. We observed an increased gene expression of MnSOD and TRX1 when DKC1 and NOP10 were silenced, which suggests a counteracting response to oxidative stress to attenuate oxidative stress. However, this may occur as an immediate response for acute stress because in X-DC patients' cells, and when suffering chronic
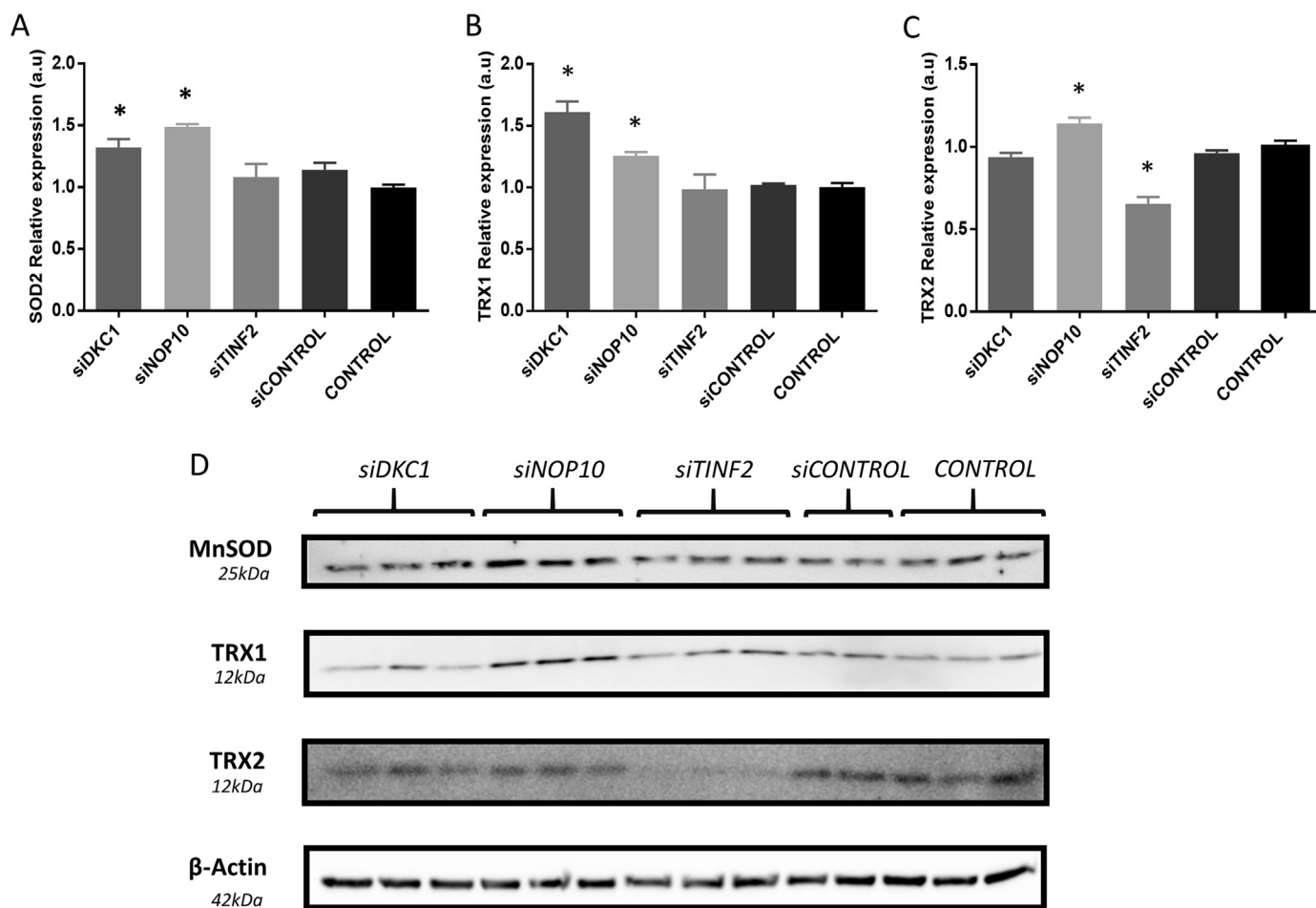
Fig. 4. Analysis of the principal antioxidant enzymes in the silenced HeLa cells. **A)** The *SOD2* mRNA levels evaluated by RT-qPCR. **B)** The *TRX1* mRNA levels evaluated by RT-qPCR. **C)** The *TRX2* mRNA levels evaluated by RT-qPCR. The expression was compared to *GAPDH* as a gene for normalization. Bars represent the mean ± SD of three independent experiments and statistical significance refers to the value of the CONTROL samples under each condition (*p < 0.05). **D)** The Western blot analysis of MnSOD, TRX1 and TRX2. The expression was compared to β-Actin as a protein for normalization (Densitometry data are shown in Supplementary Fig. S3). There were three independent experiments per group.

oxidative stress, antioxidant enzymes were down-regulated [33,36]. In fact the antioxidant response seems to depend on the chronicity of the disease and the pleiotropic effects produced by chronic oxidative stress [53]. Based on the concepts of Villeneuve et al., under mild or acute oxidative stress conditions, cells activate Nrf2 and downstream antioxidant genes (i.e. catalase, MnSOD, etc.), which occurred in our siRNA models. However, chronic oxidative stress and its derived pleiotropic effects may alter many cellular signals and mechanisms, such as antioxidant defence, DDR, senescence and apoptosis, which occurs in the cells that derive from patients. This could agree with the results obtained for siTINF2 cells, for which we found no pro-oxidant status. However, it has been proposed in the cells that carry TIN2 mutations that a pro-oxidant environment is the result of DDR initiated by telomerase deficiency and subsequent telomere shortening [15].

Yet despite finding oxidative stress in the siDKC1 and siNOP10 cells, we detected no changes in cellular viability and cell cycle, nor any significant differences in the γ-H2A.X foci, not even after exposure to H_2O_2. Probably because the number of double strand breaks (DSBs) in DNA may be still very small at 48 h of cell culture [33,54], or DDR could be impaired in these cellular models. Another possibility is that treatment with H_2O_2 causes many single-strand breaks (SSB), but only a few γ-H2A.X foci [55], which is probably because the timely repair of one-strand lesions prevents the subsequent formation of DSBs [56]. In fact high levels of γ-H2A.X in the cells of DC patients [15,33] have suggested that these cells accumulate DNA damage marks over time.

We also evaluated the effects of gene depletion on DDR with

measurements of PARylation levels. PARylation is a pivotal post-translational protein modification (PTM) that appears rapidly at DNA damage sites. It may be activated by both SSBs and DSBs, which serve as scaffolds to recruit repairing machineries (base excision repair and alternative/back-up non homologous end joining (A-NHEJ)) [57]. In spite of not finding changes in the PARylation levels under the basal conditions, high protein PARylation values were detected in the etoposide-treated siDKC and siNOP10 cells. These results indicate that the silenced cells for DKC1 and NOP10 are more susceptible to DNA damage than the siTINF2 cells or, in any case, that the siTINF2 cells are less able to signal SSBs.

No universal agreement about the role of DC mutations in the DNA damage response has been reached. Gu et al. have reported that pathogenic Dkc1 mutations in mice cause an enhanced DNA damage response in normal-length telomeres [54,58]. Conversely, mouse models with mutations Terc and Tert have displayed a normal response [54,58]. A DDR decrease in siDKC1 colorectal cancer cells has also been observed [59]. The transient siRNA-mediated depletion of DKC1 and NOP10 also limits DNA damage accumulation in human U2OS osteosarcoma cells [31]. As regards DC patients' cells, which bear DKC1, TERC and TERT mutations, some authors have found that DDR does not increase [54,58], while others have reported high levels of DDR [33], which stresses the scarce comprehension of these mechanisms in DC.

Our results agree with those obtained by Lin, Mobasher and Alawi [31] because we did not detect any changes in DDR after the siRNA-mediated depletion of DKC1, NOP10 or TINF2. This finding indicates
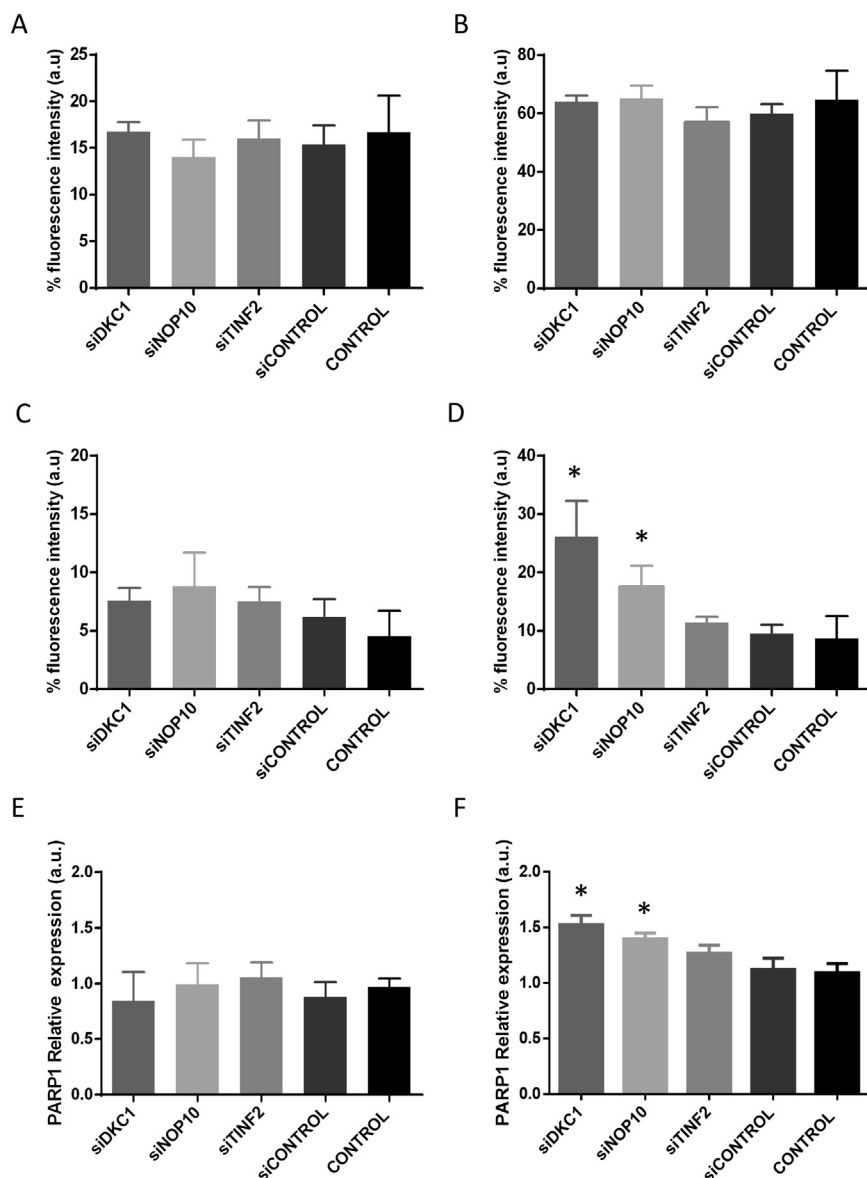
Fig. 5. Analysis of the principal DNA damage parameters in the silenced HeLa cells. **A)** The γ-H2A.X basal levels measured by flow cytometry. **B)** The γ-H2A.X levels in different cells models after DNA damage induction by H_2O_2. **C)** The PARylation basal levels measured by flow cytometry. **D)** The PARylation levels in the cell models after DNA damage induction by etoposide. **E)** The *PARP1* mRNA basal levels evaluated by RT-qPCR. **F)** The *PARP1* mRNA levels evaluated by RT-qPCR after DNA damage induction by etoposide. Relative expression levels for PARP1 in Fig. 5F for each cell line were calculated using control condition in basal levels showed in Fig. 5E. The expression was compared to *GAPDH* as a gene for normalization. The results are represented as arbitrary units (a.u.) and are expressed as fluorescence intensity. Bars represent the mean ± SD of three independent experiments and statistical significance refers to the value of the CONTROL samples under each condition (*p < 0.05).

that DDR dysregulation and accumulation of DNA damage may accumulate over time as a cause of increased oxidative stress, which may be considered a primary event in DC, specifically for mutations DKC1 and NOP10.

The main conclusion drawn from our study is that acute DKC1 and NOP10 depletion disrupts the RNA maturation process and triggers oxidative stress as an early event and one independent of telomere shortening. Conversely, acute TIN2 depletion was unable to induce oxidative stress.

It is known that individuals with a TIN2 mutation tend to have very short telomeres. However, the mechanism by which TIN2 mutation results in telomere shortening has not yet been identified. By putting our results to good use, we propose that chronic oxidative stress, together with DNA damage accumulation in telomeres, could explain how telomeres can be shortened over time. Future studies using acute and chronic depletions of DC-related proteins may help us to understand the underlying common manifestations and features of DC, irrespectively of the mutation of origin. It appears that telomere attrition is not a primary cause of oxidative stress, and is most probably the oxidative one of the potential causes of telomere shortening in those diseases in which telomerase activity is impaired.

Author Contributions

Conception and study design: JSIC, GPM, JLGG and FVP. Experiment performing and acquisition: JSIC, MSC, EBP, and GPM.

Drafting the manuscript: GPM, JLGG, and FVP. All the authors have approved the final version of this manuscript. All the authors agree to be accountable for all aspects of the work in ensuring that any question related to the accuracy or integrity of any part of this work is appropriately investigated and resolved. All the persons designated as authors qualify for authorship, and all those who qualify for authorship are listed.

Appendix A. Supplementary material

Supplementary data associated with this article can be found in the online version at http://dx.doi.org/10.1016/j.redox.2017.10.004.

References

[1] G. Sarek, P. Marzec, P. Margalef, S.J. Boulton, Molecular basis of telomere dysfunction in human genetic diseases, Nat. Struct. Mol. Biol. 22 (2015) 867–874.

[2] H. Xin, D. Liu, Z. Songyang, The telosome/shelterin complex and its functions, Genome Biol. 9 (2008) 232.

[3] Y. Xu, A. Goldkorn, Telomere and telomerase therapeutics in cancer, Genes 7 (2016).

[4] M. Armanios, Syndromes of telomere shortening, Annu. Rev. Genom. Hum. Genet. 10 (2009) 45–61.

[5] C.A. Armstrong, K. Tomita, Fundamental mechanisms of telomerase action in yeasts and mammals: understanding telomeres and telomerase in cancer cells, Open Biol. 7 (2017).

[6] J.M. Wong, K. Collins, Telomerase RNA level limits telomere maintenance in X-linked Dyskeratosis congenita, Genes Dev. 20 (2006) 2848–2858.

[7] N.D. Nelson, A.A. Bertuch, Dyskeratosis congenita as a disorder of telomere maintenance, Mutat. Res. 730 (2012) 43–51.

[8] B.J. Ballew, M. Yeager, K. Jacobs, N. Giri, J. Boland, L. Burdett, B.P. Alter, S.A. Savage, Germline mutations of regulator of telomere elongation helicase 1, RTEL1, in Dyskeratosis congenita, Hum. Genet. 132 (2013) 473–480.

[9] I. Dokal, T. Vulliamy, P. Mason, M. Bessler, Clinical utility gene card for: Dyskeratosis congenita - update 2015, Eur. J. Hum. Genet. (23) (2015).

[10] C. Trahan, C. Martel, F. Dragon, Effects of dyskeratosis congenita mutations in dyskerin, NHP2 and NOP10 on assembly of H/ACA pre-RNPs, Hum. Mol. Genet. 19 (2010) 825–836.

[11] T. Vulliamy, R. Beswick, M. Kirwan, A. Marrone, M. Digweed, A. Walne, I. Dokal, Mutations in the telomerase component NHP2 cause the premature ageing syndrome dyskeratosis congenita, Proc. Natl. Acad. Sci. USA 105 (2008) 8073–8078.

[12] L. Pereboeva, E. Westin, T. Patel, I. Flaniken, L. Lamb, A. Klingelhutz, F. Goldman, DNA damage responses and oxidative stress in dyskeratosis congenita, PLoS One 8 (2013) e76473.

[13] L.B. Sullivan, J.H. Santos, N.S. Chandel, Mitochondria and telomeres: the promiscuous roles of TIN2, Mol. Cell 47 (2012) 823–824.

[14] L.Y. Chen, Y. Zhang, Q. Zhang, H. Li, Z. Luo, H. Fang, S.H. Kim, L. Qin, P. Yotnda, J. Xu, B.P. Tu, Y. Bai, Z. Songyang, Mitochondrial localization of telomeric protein TIN2 links telomere regulation to metabolic control, Mol. Cell 47 (2012) 839–850.

[15] L. Pereboeva, M. Hubbard, F.D. Goldman, E.R. Westin, Robust DNA damage response and elevated reactive oxygen species in TINF2-mutated Dyskeratosis congenita cells, PLoS One 11 (2016) e0148793.

[16] E.R. Westin, N. Aykin-Burns, E.M. Buckingham, D.R. Spitz, F.D. Goldman, A.J. Klingelhutz, Thep53/p21(WAF/CIP) pathway mediates oxidative stress and senescence in dyskeratosis congenita cells with telomerase insufficiency, Antioxid. Redox Signal 14 (2011) 985–997.

[17] K. von Stedingk, J. Koster, M. Piqueras, R. Noguera, S. Navarro, S. Pahlman, R. Versteeg, I. Ora, D. Gisselsson, D. Lindgren, H. Axelson, snoRNPs regulate telomerase activity in neuroblastoma and are associated with poor prognosis, Transl. Oncol. 6 (2013) 447–457.

[18] B.W. Gu, J.M. Fan, M. Bessler, P.J. Mason, Accelerated hematopoietic stem cell aging in a mouse model of dyskeratosis congenita responds to antioxidant treatment, Aging Cell 10 (2011) 338–348.

[19] K. Kurvinen, S. Syrjanen, B. Johansson, Long-term suppression of telomerase expression in HeLa cell clones, transfected with an expression vector carrying siRNA targeting hTERT mRNA, Int. J. Oncol. 29 (2006) 279–288.

[20] F. Alawi, P. Lin, Dyskerin is required for tumor cell growth through mechanisms that are independent of its role in telomerase and only partially related to its function in precursor rRNA processing, Mol. Carcinog. 50 (2011) 334–345.

[21] L. Iarriccio, C. Manguan-Garcia, L. Pintado-Berninches, J.M. Mancheno, A. Molina, R. Perona, L. Sastre, GSE4, a small Dyskerin- and GSE24.2-related peptide, induces telomerase activity, cell proliferation and reduces DNA damage, oxidative stress and cell senescence in Dyskerin mutant cells, PLoS One 10 (2015) e0142980.

[22] K.J. Livak, T.D. Schmittgen, Analysis of relative gene expression data using real-time quantitative PCR and the 2(-Delta Delta C(T)) Method, Methods 25 (2001) 402–408.

[23] B.J. Olson, Assays for determination of protein concentration, Curr. Protoc. Pharmacol. 73 (2016) (A 3A 1 A 3A 32).

[24] R.M. Cawthon, Telomere length measurement by a novel monochrome multiplex quantitative PCR method, Nucleic Acids Res. 37 (2009) e21.

[25] E. Shacter, J.A. Williams, M. Lim, R.L. Levine, Differential susceptibility of plasma proteins to oxidative modification: examination by western blot immunoassay, Free Radic. Biol. Med. 17 (1994) 429–437.

[26] A. Kunzmann, D. Liu, K. Annett, M. Malaise, B. Thaa, P. Hyland, Y. Barnett, A. Burkle, Flow-cytometric assessment of cellular poly(ADP-ribosyl)ation capacity in peripheral blood lymphocytes, Immun. Ageing 3 (2006) 8.

[27] L. Rocchi, A.J. Barbosa, C. Onofrillo, A. Del Rio, L. Montanaro, Inhibition of human dyskerin as a new approach to target ribosome biogenesis, PLoS One 9 (2014) e101971.

[28] B. Holohan, W.E. Wright, J.W. Shay, Cell biology of disease: Telomeropathies: an emerging spectrum disorder, J. Cell Biol. 205 (2014) 289–299.

[29] D.M. Townsley, B. Dumitriu, N.S. Young, Bone marrow failure and the telomeropathies, Blood 124 (2014) 2775–2783.

[30] M. Fumagalli, F. Rossiello, M. Clerici, S. Barozzi, D. Cittaro, J.M. Kaplunov, G. Bucci, M. Dobreva, V. Matti, C.M. Beausejour, U. Herbig, M.P. Longhese, F. d'Adda di Fagagna, Telomeric DNA damage is irreparable and causes persistent DNA-damage-response activation, Nat. Cell Biol. 14 (2012) 355–365.

[31] P. Lin, M.E. Mobasher, F. Alawi, Acute dyskerin depletion triggers cellular senescence and renders osteosarcoma cells resistant to genotoxic stress-induced apoptosis, Biochem. Biophys. Res. Commun. 446 (2014) 1268–1275.

[32] J. Carrillo, A. Gonzalez, C. Manguan-Garcia, L. Pintado-Berninches, R. Perona, p53 pathway activation by telomere attrition in X-DC primary fibroblasts occurs in the absence of ribosome biogenesis failure and as a consequence of DNA damage, Clin. Transl. Oncol. 16 (2014) 529–538.

[33] C. Manguan-Garcia, L. Pintado-Berninches, J. Carrillo, R. Machado-Pinilla, L. Sastre, C. Perez-Quilis, I. Esmoris, A. Gimeno, J.L. Garcia-Gimenez, F.V. Pallardo, R. Perona, Expression of the genetic suppressor element 24.2 (GSE24.2) decreases DNA damage and oxidative stress in X-linked dyskeratosis congenita cells, PLoS One 9 (2014) e101424.

[34] E. Fouquerel, J. Lormand, A. Bose, H.T. Lee, G.S. Kim, J. Li, R.W. Sobol, B.D. Freudenthal, S. Myong, P.L. Opresko, Oxidative guanine base damage regulates human telomerase activity, Nat. Struct. Mol. Biol. 23 (2016) 1092–1100.

[35] C. Correia-Melo, G. Hewitt, J.F. Passos, Telomeres, oxidative stress and inflammatory factors: partners in cellular senescence? Longev. Healthspan 3 (2014) 1.

[36] G. Perez-Rivero, M.P. Ruiz-Torres, M.L. Diez-Marques, A. Canela, J.M. Lopez-Novoa, M. Rodriguez-Puyol, M.A. Blasco, D. Rodriguez-Puyol, Telomerase deficiency promotes oxidative stress by reducing catalase activity, Free Radic. Biol. Med. 45 (2008) 1243–1251.

[37] T.C. Pereboom, L.J. van Weele, A. Bondt, A.W. MacInnes, A zebrafish model of dyskeratosis congenita reveals hematopoietic stem cell formation failure resulting from ribosomal protein-mediated p53 stabilization, Blood 118 (2011) 5458–5465.

[38] B.T.K. Kaymaz, B., Advances in therapeutic approaches using RNA interference as a gene silencing tool, Adv. Tech. Biol. Med. 1 (2013).

[39] P. Lin, M.E. Mobasher, Y. Hakakian, V. Kakarla, A.F. Naseem, H. Ziai, F. Alawi, Differential requirements for H/ACA ribonucleoprotein components in cell proliferation and response to DNA damage, Histochem. Cell Biol. 144 (2015) 543–558.

[40] I. Dokal, Dyskeratosis congenita, Hematol. Am. Soc. Hematol. Educ. Program 2011 (2011) 480–486.

[41] E.F. Freed, F. Bleichert, L.M. Dutca, S.J. Baserga, When ribosomes go bad: diseases of ribosome biogenesis, Mol. Biosyst. 6 (2010) 481–493.

[42] A. Yoon, G. Peng, Y. Brandenburger, O. Zollo, W. Xu, E. Rego, D. Ruggero, Impaired control of IRES-mediated translation in X-linked dyskeratosis congenita, Science 312 (2006) 902–906.

[43] G. Glousker, F. Touzot, P. Revy, Y. Tzfati, S.A. Savage, Unraveling the pathogenesis of Hoyeraal-Hreidarsson syndrome, a complex telomere biology disorder, Br. J. Haematol. 170 (2015) 457–471.

[44] S. Yang, C.M. Counter, Cell cycle regulated phosphorylation of the telomere-associated protein TIN2, PLoS One 8 (2013) e71697.

[45] M. Kirwan, R. Beswick, T. Vulliamy, A.C. Nathwani, A.J. Walne, C. Casimir, I. Dokal, Exogenous TERC alone can enhance proliferative potential, telomerase activity and telomere length in lymphocytes from dyskeratosis congenita patients, Br. J. Haematol. 144 (2009) 771–781.

[46] T. Vulliamy, R. Beswick, M.J. Kirwan, U. Hossain, A.J. Walne, I. Dokal, Telomere length measurement can distinguish pathogenic from non-pathogenic variants in the shelterin component, TIN2, Clin. Genet. 81 (2012) 76–81.

[47] D. Frescas, T. de Lange, A TIN2 dyskeratosis congenita mutation causes telomerase-independent telomere shortening in mice, Genes Dev. 28 (2014) 153–166.

[48] D. Yang, Q. He, H. Kim, W. Ma, Z. Songyang, TIN2 protein dyskeratosis congenita missense mutants are defective in association with telomerase, J. Biol. Chem. 286 (2011) 23022–23030.

[49] L. Montanaro, M. Brigotti, J. Clohessy, S. Barbieri, C. Ceccarelli, D. Santini, M. Taffurelli, M. Calienni, J. Teruya-Feldstein, D. Trere, P.P. Pandolfi, M. Derenzini, Dyskerin expression influences the level of ribosomal RNA pseudo-uridylation and telomerase RNA component in human breast cancer, J. Pathol. 210 (2006) 10–18.

[50] A. Henras, Y. Henry, C. Bousquet-Antonelli, J. Noaillac-Depeyre, J.P. Gelugne, M. Caizergues-Ferrer, Nhp2p and Nop10p are essential for the function of H/ACA snoRNPs, EMBO J. 17 (1998) 7078–7090.

[51] R. Machado-Pinilla, D. Liger, N. Leulliot, U.T. Meier, Mechanism of the AAA+ ATPases pontin and reptin in the biogenesis of H/ACA RNPs, RNA 18 (2012) 1833–1845.

[52] A.B. Fisher, Peroxiredoxin 6: a bifunctional enzyme with glutathione peroxidase and phospholipase A(2) activities, Antioxid. Redox Signal 15 (2011) 831–844.

[53] N.F. Villeneuve, Z. Sun, W. Chen, D.D. Zhang, Nrf2 and p21 regulate the fine balance between life and death by controlling ROS levels, Cell Cycle 8 (2009) 3255–3256.

[54] M. Kirwan, R. Beswick, A.J. Walne, U. Hossain, C. Casimir, T. Vulliamy, I. Dokal, Dyskeratosis congenita and the DNA damage response, Br. J. Haematol. 153 (2011)

634–643.

[55] M. Lobrich, A. Shibata, A. Beucher, A. Fisher, M. Ensminger, A.A. Goodarzi, O. Barton, P.A. Jeggo, gammaH2AX foci analysis for monitoring DNA double-strand break repair: strengths, limitations and optimization, Cell Cycle 9 (2010) 662–669.

[56] T. Mahaseth, A. Kuzminov, Prompt repair of hydrogen peroxide-induced DNA lesions prevents catastrophic chromosomal fragmentation, DNA Repair 41 (2016) 42–53.

[57] C. Beck, I. Robert, B. Reina-San-Martin, V. Schreiber, F. Dantzer, Poly(ADP-ribose) polymerases in double-strand break repair: focus on PARP1, PARP2 and PARP3, Exp. Cell Res. 329 (2014) 18–25.

[58] B.W. Gu, M. Bessler, P.J. Mason, A pathogenic dyskerin mutation impairs proliferation and activates a DNA damage response independent of telomere length in mice, Proc. Natl. Acad. Sci. USA 105 (2008) 10173–10178.

[59] R. T.J. Ting, R. Harun, W.Z. Ngah, N.M. Mokhtar, RNA interference-mediated knockdown on DKC1 gene in chemosensitized colorectal cancer cell lines, Int. J. Cancer Res. Mol. Mech. 1 (2) (2015).